

SURFACE DUST REDISTRIBUTION ON MARS FROM INTERANNUAL DIFFERENCES IN TEMPERATURES AND ALBEDO

J. Bapst (jonathan.bapst@jpl.nasa.gov), **S. Piqueux**, **D.M. Kass**, **A. Kleinböhl**, *Jet Propulsion Laboratory, California Institute of Technology, Pasadena, USA*, **C.S. Edwards**, **C. Wolfe**, *Northern Arizona University, Flagstaff, USA*, **P.O. Hayne**, *University of Colorado, Boulder, USA*.

Introduction: The focus of this work is to advance our understanding of the impact of global dust storms (GDS) on the state of dust reservoirs because of their propensity for dust lifting and redistribution [1-4]. Mapping the global distribution of surface dust, and identifying dust reservoirs has been carried out previously using derived albedo [6,1], visible imagery [7,8,3,9], and dust cover index derived from infrared spectra [10].

Outstanding questions pertain to dust fluxes and include whether replenishing of dust reservoirs is necessary for GDS initiation (i.e., “*are dust source regions exhausted during GDSs?*”). General Circulation Models (GCM) initialized with a finite supply of surface dust show that source regions will be quickly depleted and inhibit dust storm activity [11]. This is not consistent with observations [12]. Thus, [11] concluded that source regions are large reservoirs, providing dust for lifting on at least multi-decadal timescales, and that the interannual variability in dust storms is not due to availability of surface dust. Another hypothesis is that dust must be deposited or removed in certain geographic locations to explain interannual variability of GDS [13].

Approach: We identify the location of dust sources and sinks and study their changes before and after GDS. We leverage the nearly continuous and global surface temperature record available at Mars. Orbital measurements of surface temperature spanning 10 Mars Years (MY), along with less-complete albedo datasets, are used as proxies for surface dust distribution, allowing us to track changes across Mars through time. The high sensitivity of those measurements provides a different and complimentary perspective into dust redistribution that is not possible using visible datasets alone.

Our approach primarily involves the analysis and identification of temperature changes from one Mars year to the next. Martian dust is characterized by its relatively high albedo (>0.25 ; [6,14]) and low thermal inertia ($20\text{--}100\text{ J m}^{-2}\text{ K}^{-1}\text{ s}^{-1/2}$), in contrast to the rest of the surface which, besides ices that exhibit high albedo value, is characterized by lower albedo (<0.25) and has thermal inertia values between $100\text{--}400\text{ J m}^{-2}\text{ K}^{-1}\text{ s}^{-1/2}$ [15,16]. Owing to differences between dust and other surface types, the redistribution of surface dust can result in changes in albedo and/or

thermal insulation, which affects surface temperature via surface-energy balance [17,6,1]. Therefore, surface temperatures changes can help us understand the spatial and temporal nature of dust redistribution.

To study dust redistribution globally, we consider two instrument datasets: Thermal Emission Spectrometer (TES [14]) aboard Mars Global Surveyor and Mars Climate Sounder (MCS [18]) aboard Mars Reconnaissance Orbiter. TES and MCS data are binned in an identical manner. Data are separated by local time into AM ($<12\text{ PM}$) and PM ($>12\text{ PM}$). We divide the data by season into 15° L_S windows, which is necessary when carrying out difference operations as seasonal differences will dominate for larger L_S windows. An L_S window of 15° provided the best spatial coverage while limiting the seasonal influence on temperature at $1^\circ\times 1^\circ$ latitude by longitude spatial resolution. To achieve a more-complete map concerning data density, we average (median) a full season (90° of L_S or six 15° maps) of data after calculating interannual differences. Analysis is limited below 60° latitude in both hemispheres. Temperatures at higher latitudes should be interpreted with caution, as they are subject to variable presence of seasonal surface frosts [19,20], subsurface frost with the potential for gardening [21], and enhanced aerosol and condensate loading in the atmosphere (i.e., polar hoods).

Following binning, interannual difference maps of temperature and albedo are generated and averaged over a larger seasonal baseline (90° of L_S) for analysis. These changes in surface temperature and albedo are interpreted in terms of dust redistribution; i.e., AM temperatures would decrease with dust deposition as it would increase albedo and lower the effective surface thermal inertia. Geographical naming convention follows [8].

MY25 GDS: Interannual changes in albedo before and after the MY25 GDS exhibit the largest and most extensive changes throughout the TES observations included in our analysis. Extensive areas of change are observed south of the Tharsis province (10°N , -120°E) in Daedalia Planum (-25°N , -110°E), south of Valles Marinaris (-10°N , -70°E) in Solis Planum (-25°N , -75°E), in and around Hellas Planitia (-45°N , 70°E), and in Syrtis Major (10°N , 70°E)—all consistent with findings from previous studies [8,1,3].

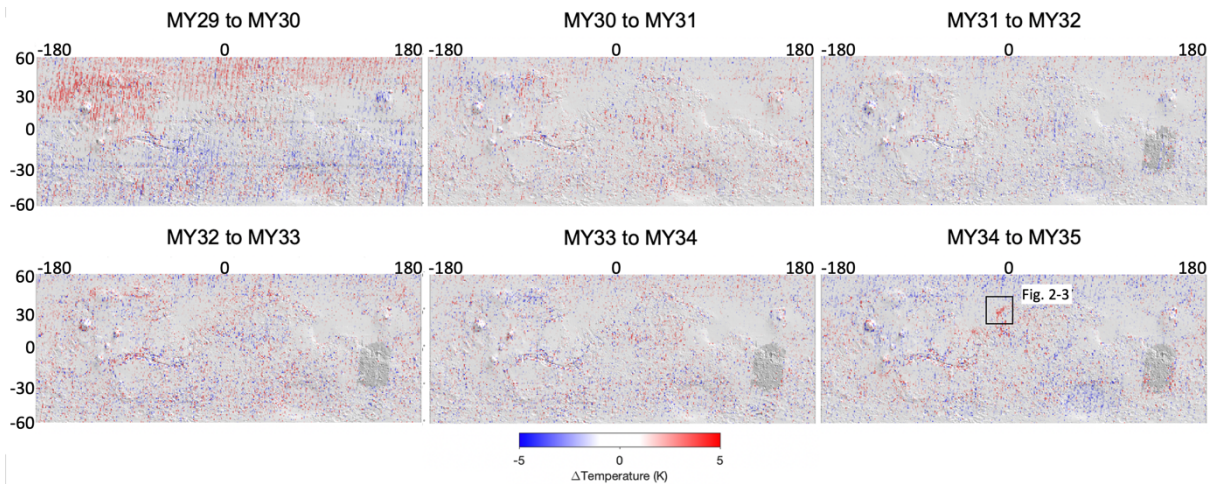


Figure 1: Global map of MCS AM surface temperature change, $L_s=0^\circ-90^\circ$. Note the lack of data coverage near Gale Crater in MY31 and after.

We see excellent agreement between the location of albedo changes and inversely corresponding changes in surface temperature. We would expect the strongest agreement with albedo change in PM data, due to the local time dependency. Compared to albedo, changes observed in PM temperatures are not as clearly defined and are more susceptible to orbit-to-orbit variability than albedo changes.

AM surface temperature changes display a similar pattern, and the geographic extent of the changes are in good agreement. One major difference is that AM temperature changes are the same sign but are less than half the magnitude of those changes observed in PM. Because the magnitude of AM changes is less than PM changes (i.e., smaller signal), the AM maps are more susceptible to small changes that do not represent surface dust redistribution. The similarities between interannual PM and AM surface temperatures changes bracketing the MY25 GDS are noteworthy because both AM and PM surface temperature changes inversely correlate with albedo. This implies that changes in temperature are driven primarily by changing surface albedo opposed to the insulating effects of dust.

Overall, the interannual changes for the pair of years beyond the MY25 GDS show albedo and temperature changes smaller in magnitude compared to the years surrounding the GDS. Changes in albedo supports the idea that the surface may require more than one Mars year to return to a MY24-like or “pre-storm” state. Surface temperatures show the same behavior and do not invert over the course of one MY.

MY28 GDS: No TES or MCS surface observations are available before and after the MY28 GDS, but substantial changes in AM temperature are observed in MY29 and MY30, Fig. 1. Persistent temperature changes in the region east of Valles Marineris and north of Tharsis could be due to atmospheric activity such as water ice clouds [22].

MY29 to MY30, show substantial changes in temperature, most notably north and northwest of Tharsis in Amazonis Planitia. [3] identify a spatially-

coincident change in reflectance in this region between global mosaics between MY29 and MY27. This is consistent with dust deposition in this region about the MY28 GDS. Because our analysis brackets the years directly following the MY28 GDS (i.e., MY29 to MY30) we would expect a decrease in albedo and thus a positive temperature change. This was observed in the years following the MY25 GDS, in regions where dust was initially deposited during the storm (e.g., Hellas Planitia).

MY34 GDS: A positive temperature change identified in the AM temperature map bracketing the MY34 GDS suggests a decrease in albedo and/or an increase in the effective thermal inertia, both consistent with dust removal. Although we do not have simultaneous, coincident observations of broadband albedo, observed changes in temperature guide us towards visible (or other) datasets that may corroborate the temperature changes (Fig. 2). This region, along the border of Arabia and Acidalia, is a well-documented storm track [23,24] where substantial changes in albedo have been observed over decades of monitoring [3,9].

Two MRO Context Camera (CTX [25]) images bracket the MY34 GDS in this region of observed change and share almost exactly the same viewing geometry (Fig. 2)—The latter restriction is employed to rule out explanations, besides dust redistribution, for the observed changes between images. A pair of images captured by the High-Resolution Imaging Science Experiment (HiRISE; [26]), with similar viewing geometries, are also identified (Fig. 2). Visible images capture clear evidence for dust removal about the MY34 GDS, located in the broad region of AM temperature change identified in MCS data within NW Arabia Terra. The “before” scenes show brightness is primarily a function of incidence angle (i.e., slope). West-facing slopes receive more solar flux (~3 PM local time), but have similar reflectance properties, and are therefore brighter in the image. The “after” scenes are markedly different, where brightness corresponds to local topographic highs and visible surface roughness. The eroded rim

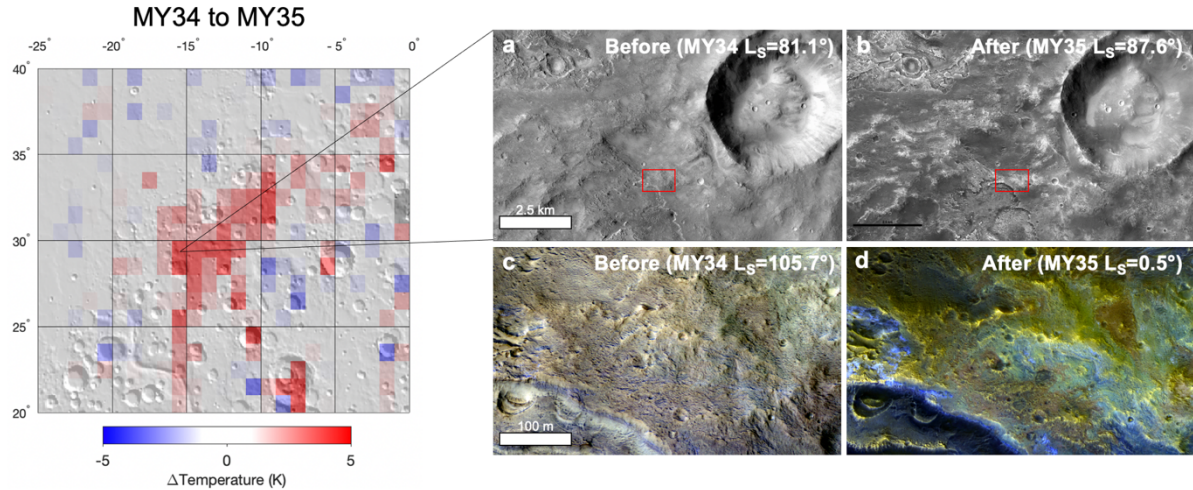


Figure 2: (left) Regional view of the positive temperature anomaly (See Fig. 1). Temperature changes $< \pm 2$ K are omitted from view. CTX view of a region in NW Arabia Terra (a) before and (b) after the MY34 GDS. Stretched HiRISE color images (red outline) show stark differences in the color information (c) before and (d) after the MY34 GDS. CTX IDs from left to right are J20_052788_2109_XI_30N016W and K22_061795_2095_XI_29N015W, and for HiRISE, ESP_053500_2095 and ESP_059329_2095, respectively. North is up.

of the larger crater is bright as well as the rim of the smaller crater in the scene. This difference suggests that dust in smooth or flat-lying regions of the scene was removed in the time between images (i.e., MY34 GDS), resulting in a net decrease in albedo (and potentially net-increase in thermal inertia) and therefore a net-increase in temperature, consistent with our MCS observations. CTX images bracketing the MY34 GDS were also identified in the region that did not overlap with MCS temperature changes and did not show clear evidence for surface changes.

Implications for the dust cycle: One outstanding question is whether surface dust reservoirs are finite in volume and need to be resupplied for GDS to occur [15] or have a virtually unlimited dust volume (i.e., deep reservoir). Our results for MY25 GDS are partially ambiguous due to the start of observations of MGS and the lack of data before the GDS. The first useful interannual changes are after the global event has occurred. The changes in years following the MY25 GDS mostly support a return to “pre-storm” conditions, supporting a finite reservoir that needs resupply before another GDS can initiate. However, the magnitude of change (in albedo and temperature) is smaller than those across the years directly following the storm. Some regions appear not to revert or are doing so slowly (e.g., Daedalia and Tharsis), likely requiring a GDS-like event, or multiple years—or both—to return to a prior state, if at all [7,1]. These observations support the deep reservoir model, where dust is available in quasi-unlimited supply.

MCS observations support the deep reservoir model as no large changes or systematic changes over time are observed in the leadup to the MY34 GDS. In particular, the region showing the strongest evidence for dust removal, NW Arabia Terra, showed no

significant interannual changes in AM temperature for the previous five Mars Years. Thus, results suggest replenishment of well identified discrete dust source regions is not necessary for initiating GDS.

Using a thermal model to quantify the amount of dust necessary to fit the observed temperature changes, the MY25 interannual changes in AM and PM temperature are consistent with dust layer thickness changes < 100 – 1000 microns as an upper limit, and down to 5 – 10 microns of dust displacement as a lower limit based on the interpretation of albedo changes. Results support the notion that dust can significantly impact albedo, requiring only addition or removal on the order of monolayers, while having a negligible impact on surface thermal properties [5]. These observations support a deep reservoir for dust sources, insofar regions of dust are known to be at least decimeters thick and potential many 10s of meters thick [27]. Annual or interannual removal of surface layers on the upper end of our estimates (~ 100 microns) implies dust reservoir lifetimes of at least 10^3 years and potentially much longer.

Laboratory work by [5] linking albedo changes to dust deposition thickness can provide a lower limit of the total mass of dust transported globally about GDSs. This quantity, summed across the entire surface about the MY25 GDS equates to 8.0×10^{10} kg of dust removed and 5.8×10^{10} kg dust deposited calculated over one Mars year. The values imply at least 8.0×10^{10} kg of dust involved in transport about the storm. Comparing this to historical estimates of dust flux supports this value as a lower limit. For example, [28] estimate from Viking Orbiter data a yearly dust flux of 2.9×10^{12} kg about the MY13 GDS (1977). [29] estimates 4.3×10^{11} kg of dust as peak atmospheric loading of the same storm with Viking Orbiter data. [30] report 5.0×10^{11} kg of surface dust

annually transported. The estimated flux of dust lifted by dust devils are of similar magnitude as other reported estimates, where between $2.3\text{--}5.8 \times 10^{11}$ kg of dust is lifted annually (limits reported by [31] and [8], respectively).

Although we have not derived quantitative albedo from MCS visible channel observations to support calculations of dust flux directly, as was performed with TES data, we can calculate the local dust flux from the region in NW Arabia where we identified dust removal and estimated albedo changes (Fig. 3). Following the same approach as performed with TES albedo, we sum the dust thickness change across the region of interest. This equates to 5.4×10^8 kg of dust, roughly 2–3 orders of magnitude less than the global transported mass during other GDS, and notably less than the flux estimated for a regional storm in [29]— 1.3×10^{10} kg. Again, comparing our results to those in the literature suggests our model may be too sensitive (i.e., the required dust mass to effect albedo change is larger than what we assume) and/or the assumption of uniform layers being added or removed at the spatial resolution of our analysis is unrealistic (e.g., [32,6]). Allowing for heterogeneous dust addition/removal (i.e., non-uniformity or sub-pixel variability), and

thus thicker quantities of dust than what we estimate, is one potential explanation, however there is no evidence these thicknesses are significant in terms of affecting insulating properties of the surface.

Differences between observations about the MY25 GDS and MY34 GDS are substantial. Dust redistribution across the MY25 event results in clear changes in both PM and AM temperatures while AM temperature changes are less pronounced across the MY34 GDS. One potential cause is the areal extent of dust removed between the two GDSs. Interannual temperature changes about the MY25 GDS showed broad areas of substantial dust removal across the Tharsis Plateau and Daedalia Planum whereas in MY34, only a localized region of substantial dust lifting was identified in northwest Arabia Terra. Annual storm activity has been reported along the border of Chryse Planitia and Arabia Terra (i.e., Acidalia storm track; [8,33] but was likely more impactful in the MY34 GDS than the MY25 GDS. These observations support spatial variability between GDSs and the inclusion or exclusion of dust reservoirs that play a major role in the global event.

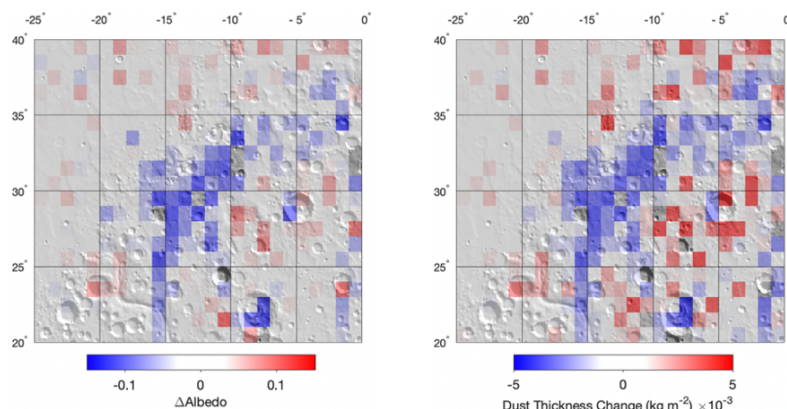


Figure 3: AM MCS temperature change from MY34 to MY35 ($0 < L_s < 90$) interpreted in terms of surface albedo variation (left) and corresponding dust thickness using [5], right. Assuming a bulk dust density of $1,000 \text{ kg m}^{-3}$, a dust thickness change of $5 \times 10^{-3} \text{ kg m}^{-2}$ is equivalent to a surficial dust layer thickness of $\sim 5 \text{ }\mu\text{m}$.

Acknowledgements: Part of this work was performed at the Jet Propulsion Laboratory, California Institute of Technology, under a contract with NASA. US government support acknowledged.

References: [1] M. A. Szwast *et al.*, *Journal of Geophysical Research* **111** (2006). [2] B. A. Cantor *et al.*, *Journal of Geophysical Research* **111** (2006). [3] P. E. Geissler *et al.*, *Icarus* **278**, 279 (2016). [4] T. Bertrand *et al.*, *Journal of Geophysical Research-Planets* **125**, 36, e2019JE006122 (2020). [5] E. N. Wells *et al.*, *Icarus* **58**, 331 (1984). [6] P. R. Christensen, *Journal of Geophysical Research* **93**, 7611 (1988). [7] P. E. Geissler, *Journal of Geophysical Research* **110** (2005). [8] B. A. Cantor, *Icarus* **186**, 60 (2007). [9] D. F. Wellington and J. F. Bell, *Icarus* **349**, 25, 113766 (2020). [10] S. W. Ruff and P. R. Christensen, *Journal of Geophysical Research* **107** (2002). [11] M. A. Kahre *et al.*, *Geophysical Research Letters* **32**, L20204 (2005). [12] R. W. Zurek and L. J. Martin, (*Amer Geophysical Union*, 1993), pp. 3247. [13] D. P. Mulholland *et al.*, *Icarus* **223**, 344 (2013). [14] P. R. Christensen *et al.*, *Journal of Geophysical Research* **106**, 23 (2001). [15] F. D. Palluconi and H. H. Kieffer, *Icarus* **45**, 415 (1981).

[16] N. E. Putzig and M. T. Mellon, *Icarus* **191**, 68 (2007). [17] H. H. Kieffer *et al.*, *Journal of Geophysical Research* **82**, 4249 (1977). [18] D. J. McCleese *et al.*, *Journal of Geophysical Research* **112** (2007). [19] J. Bapst *et al.*, *Icarus* **260**, 396 (2015). [20] S. Piqueux *et al.*, *Icarus* **251**, 164 (2015). [21] C. Pilonget and F. Forget, *Nature Geoscience* **9**, 65 (2016). [22] M. D. Smith, *Icarus* **202**, 444 (2009). [23] H. Q. Wang and M. I. Richardson, *Icarus* **251**, 112 (2015). [24] M. Battalio and H. Q. Wang, *Icarus* **354**, 20, 114059 (2021). [25] M. C. Malin *et al.*, *Journal of Geophysical Research* **112**, S504 (2007). [26] A. S. McEwen *et al.*, *Journal of Geophysical Research* **112**, E05S02 (2007). [27] P. R. Christensen, *Journal of Geophysical Research* **91**, 3533 (1986). [28] J. B. Pollack *et al.*, *Journal of Geophysical Research* **84**, 2929 (1979). [29] T. Z. Martin, *Journal of Geophysical Research* **100**, 7509 (1995). [30] B. A. Cantor *et al.*, *Journal of Geophysical Research* **106**, 23653 (2001). [31] P. L. Whelley and R. Greeley, *Journal of Geophysical Research* **113** (2008). [32] P. Thomas *et al.*, *Icarus* **60**, 161 (1984). [33] D. M. Kass *et al.*, *Geophysical Research Letters* **43**, 6111 (2016).